Chemical State Analysis of Sn-Sb-O Solid Surfaces by Auger Electron Spectroscopy: Differentiation of Sb(III) and Sb(V)

Masaharu KOMIYAMA,* Mikio YOSHII,† Yoshisada OGINO,† and Takehiko ONO††
Department of Chemistry, Faculty of Liberal Arts and Education, Yamanashi University, Takeda, Kofu 400
†Department of Molecular Chemistry and Engineering, Faculty of Engineering, Tohoku University, Aramaki Aoba, Sendai 980
††Department of Applied Chemistry, University of Osaka Prefecture, Sakai 591
(Received May 12, 1992)

Chemical state analysis of Sn–Sb–O solid surfaces was performed by means of Auger electron spectroscopy (AES). Differential and numerically integrated AE spectra were curve-fitted using standard spectra obtained from pure substances. The fitting revealed, for the first time, the possibility of differentiating two antimony oxide components, Sb(III) and Sb(V), by AES. Using the AE spectral parameters obtained for these two chemical states, a correlation between the Sb AE peak positions and the average Sb oxidation number was constructed and it was applied for the determination of the average Sb oxidation state in Sn–Sb mixed oxide systems.

Tin-antimony mixed oxides have found various industrial applications. In the field of catalysis Sn–Sb mixed oxides are used for the oxidation and the ammoxidation of propylene and oxidatative dehydrogenation of butene.[1,2] Tin and antimony are also combined to make a transparent electrode material, the so-called Nesa glass,[3] in which antimony is used as a dopant to the tin oxide electrode.

In these materials it is often important to know the surface chemical states of their constituents, i.e., Sn and Sb, in order to understand the role of these components play in these materials. For such purposes Auger- and X-ray photo-electron spectroscopies (AES and XPS, respectively) have routinely been used. For tin it has been known that neither AES nor XPS can differentiate Sn(II) from Sn(IV).[4–6] Lin et al.[4] examined SnO and SnO_2 powder surfaces by AES and XPS, and found that their spectra are essentially identical. They also examined a tin foil surface which has been spontaneously oxidized and its chemical changes with ion bombardment which is expected to reduce surface Sn(IV) to Sn(0) via Sn(II) in the course of surface sputtering. They found that there exist only two spectral components during the surface changes from oxidic to metallic due to ion bombardment, indicating the inability of differentiating Sn(II) and Sn(IV) by XPS or AES. Differentiation of SnO and SnO_2 was made possible only by electron energy loss spectroscpy.[5,6]

In the case of antimony, the possibility of differentiating Sb(III) from Sb(V) in antimony oxides by XPS has been debated.[7–10] In this case the difficulty lies in the fact that the binding energies of the 3d electrons of oxidic Sb(III) and Sb(V) are very close, resulting in a broad single peak when both chemical species are present together, and also that the O 1s electron emission peak coincides with that of Sb $3d_{5/2}$.[7,9,10] Thus curve fitting the Sb XPS peak in an attempt to separate the Sb(III) contribution from that of Sb(V) is not without ambiguity. As for Sb AES, no peak analysis has been reported to our knowledge.

In the present paper we report our attempt to differentiate Sb(III) and Sb(V) by AES. In our previous XPS study of rhenium oxide[11] we showed that gradual in situ reduction of solid surfaces by ion bombardment, which occurrs concurrently with surface sputtering, and close examination of its process by XPS, lead to unambiguous identification of chemical states of multi-valent elements. Here this technique is applied to Sb and Sn oxide systems. Gradual reduction by ion bombardment of thin oxide layers formed on Sn and Sb metal surfaces were followed by AES and the obtained spectra were fitted with standard spectra. Two oxidic Sb species were differentiated by AES for the first time, and a correlation between the Sb AE peak positions and the average Sb oxidation number in Sn–Sb mixed oxide systems was obtained.

Experimental

High-purity Sn and Sb metal plates were obtained commercially and used as received. Tin and antimony oxides, SnO, Sb_2O_3, and Sb_2O_5 were also obtained commercially. The Sb_2O_5 sample showed an X-ray diffraction pattern of Sb_6O_{13}, although its surface showed the AES characteristics of Sn(V) only, as discussed later. Tin dioxide was prepared by calcining, at 800 K, a precipitate obtained by mixing $SnCl_4$ aqueous solution with aqueous ammonium solution.

Two series of Sn–Sb–O mixed oxide catalysts were prepared by coprecipitation from aqueous solutions of $SnCl_4$ and $SbCl_5$ (series A) or $SnCl_2$ and $SbCl_5$ (Series B) using aqueous ammonia, drying the resulting hydroxide mixtures at 353 K, then calcining them at 803 K. Their physical characteristics and catalytic activities have been reported elsewhere.[2]

For AES measurements, an ultrahigh-vacuum chamber,[12] equipped with a home-computerized AE spectrometer (PHI

model CMS-10-155) was used. Powder samples were pressed onto an indium plate for AES analysis. Auger spectra were normally taken at 3 keV primary electron energy and 3 eV modulation (peak to peak). For the samples that contain Sb, 3-keV electron irradiation was found to cause Sb(V) reduction to intermadiate valency, and thus when necessary 1.5 keV primary energy that does not cause such reduction was used. The AES signal from a lock-in amplifier was digitized with a 12-bit A/D converter and stored and processed with an NEC PC-9801 microcomputer. Separate XPS measurements of Sb and Sn 3d electron binding energies were also performed for most of the samples by using Shimadzu ESCA model 750.

A note should be added here, regarding the Auger kinetic energy position expressions. Commonly AE spectra are taken in a differential form,[13] and their peak energy positions are recorded at the intensity minima of the differential peaks. On the other hand if the differential peaks are integrated, as is done in this paper, or AE emissions are directly recorded, as has been previously published,[14] then it is easier to identify AE peaks at their emission maxima. These emission maxima correspond to the zero crosspoints of differential peaks, and there is no simple relation between the differential minimum and the emission (integral) maximum positions unless the peak shapes are exactly identical. Thus in this paper we indicated AE peak positions at the zero crosspoints for the differential spectra and the peak maxima for emission (integral) spectra, so as to make the comparison of AE energy positions obtained from both spectra straightforward.

Results and Discussion

Oxide Film Reduction by Ion Bombardment. Firstly, gradual reduction processes by ion bombardment of the thin oxide films spontaneously formed on the surfaces of Sb and Sn metal plates were examined by AES. For either metal, the outermost oxide layer was dominated by highest valence oxide, as confirmed by XPS. Figures 1 and 2 show the changes of Sb and Sn MNN AE spectra, respectively, as reduction proceeds with repeated ion bombardment. Here original differential AE spectra were numerically integrated, and shown as electron emission peaks for easier comparison of the peak shape changes due to the surface reduction. Energy scale for these spectra are referenced to the O KLL peak, which showed no shift during the entire measurement.

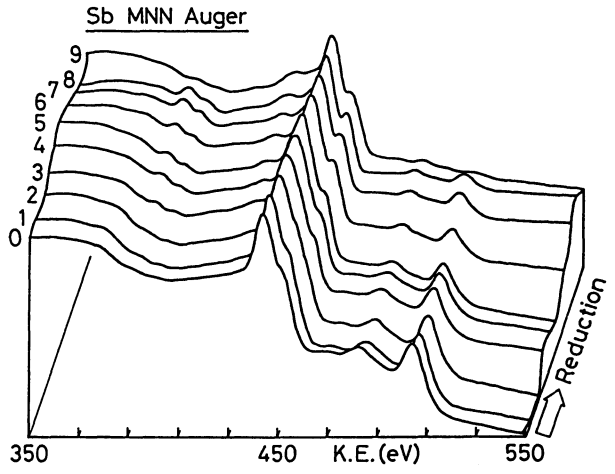

Fig. 1. Shape changes of the Sb MNN AE spectra from surface oxidized Sb metal plate as the surface is reduced by successive ion bombardment. The numbers of bombardment cycles are indicated on the left of each spectrum.

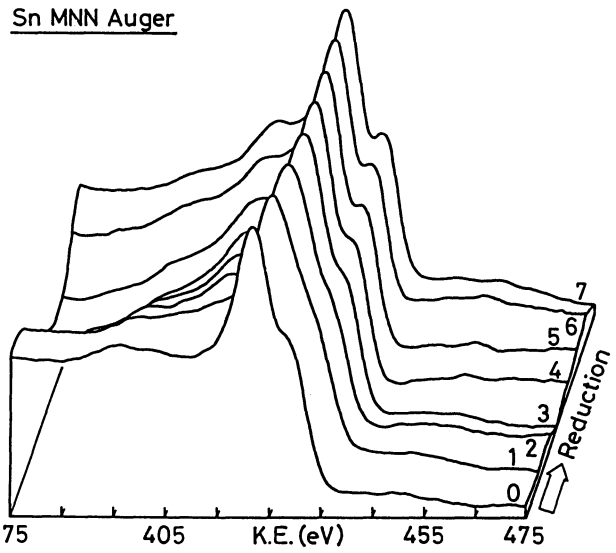

Fig. 2. Shape changes of the Sn MNN AE spectra from surface oxidized Sn metal plate as the surface is reduced by successive ion bombardment. The numbers of bombardment cycles are indicated on the right of each spectrum.

In Fig. 1, three groups of peaks may be found, in the kinetic energy ranges of 380—410, 420—460, and 470—520 eV, respectively. The first one, the doublet that appears at 380—410 eV in the intermediate region of surface reduction, is due to contaminant indium in the vacuum chamber, and its amount first increases from nil to a small amount as surface reduction proceeds with ion bombardment, and then disappears from the sample surface after prolonged bombardment. Peaks that appear in the 470—520 eV range are due to oxidic oxygen, and its amount monotonously decreases with the progress of surface reduction.

The major peak group that appears in the kinetic energy range of 420—460 eV is attributed to Sb MNN Auger emission. Three changes occur in this group of peaks as reduction by ion bombardment proceeds. Firstly, the position of the major peak, initially at 446 eV, gradually shifts toward higher kinetic energy, eventually reaching the value of 451 eV which corresponds to the differential peak minimum position of 454 eV that equals the reported $M_5N_{4,5}N_{4,5}$ kinetic energy value for metallic Sb.[13] The second change observed in this energy range is the development of a small peak, at ca. 15 eV lower to the MNN peak, which is identified as bulk plasmon loss peak associated with metallic Sb phased.[15] The relative intensity of this loss peak increases with the ion bombardment cycles, reflecting

the increase of the amount of metallic component within the surface layer. The third change apparent in the energy range is the emergence of the shoulder peak positioned on the higher kinetic energy side of the major peak as reduction proceeds. All of these three features are obviously due to the proceeding of surface reduction by ion bombardment of the surface oxide to the metallic state, and will be discussed in more detail later with spectral curve fitting.

Figure 2 shows Sn MNN Auger peak from the surface Sn oxide layer of Sn metal plate at various reduction stages caused by ion bombardment. Peak shape changes similar to those observed for Sb were also observed for Sn. In the early stages of ion bombardment the indium contamination is observed at the kinetic energy range of 380—410 eV, and it disappears quickly with successive ion bombardment. On the lower kinetic energy side of the Sn MNN peak (ca. 14 eV apart) the bulk metal plasmon loss peak[4,5,15] develops with the progress of ion bombardment. On the higher kinetic energy side the splitting of the shoulder peak with increasing ion bombardment cycles is observed. And above all the kinetic energy position of the Sn MNN peak position shifts as surface reduction proceeds, from 422 to 427 eV.

Curve Fitting of MNN Auger Spectra. In order to differentiate chemical species present on the spontaneously oxidized metal surfaces during the ion bombardment-induced surface reduction, curve fitting of each MNN Auger spectrum with standard spectra was attempted. Two fitting procedures were employed: One is the fitting of the original differential spectra, assuming that an AE spectrum obtained from multicomponent surface is a linear composit of the constituent spectra,[16,17] and the other is the fitting of the numerically integrated spectra, by assuming that each spectral component is represented by Gaussians.

First the soundness of the fitting methods employed was checked by applying them to the Sn AE spectra. Tin AE spectra was used for this purpose because Sn(II) and Sn(IV) AE spectra are known to be identical (see above) and it shows only two AE components, oxidic and metallic, during the progress of ion bombardment-induced surface reductions.[4]

Firstly, differential Sn AE spectra were fitted with two standard spectra, one obtained from SnO_2 and one from sputter-cleaned Sn metal. Following the method described by Dawson et al.,[16,17] a spectrum to be fitted is constructed by the linear combination of the two standard spectra. The only fitting parameter is the relative intensity of each spectrum. The relative intensity of each standard spectra used for the fitting, which translates to the composition of the surface layer within the Auger electron escape depth, are plotted in Fig. 3 (open symbols) as a function of ion bombardment cycles. As may be apparent in the figure, the amount of metallic tin at the surface monotonously increases at the expence of oxidic tin initially dominant on the surface as ion bombardment proceeds. This apparent surface reduction is obviously due to two factors, ion bombardment-induced surface reduction and the sputtering of the oxide away and exposing metallic surface. While the contribution of each of these two factors for the apparent surface reduction found in Fig. 3 is not known, it may be said that the overall surface reduction process appears to be rather monotonous on the Sn metal plate surface.

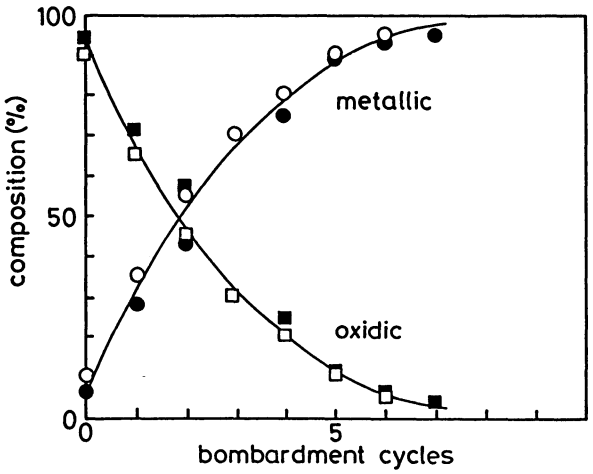

Fig. 3. Reduction behavior of spontaneously oxidized Sn metal surface by ion bombardment analyzed by the two curve fitting methods. Open symbols: differential method; closed symbols: integral method.

Curve fitting of integral AE spectra were then attempted. The procedure of the integral curve fitting is as follows. First the MNN doublets, $M_{4,5}N_{4,5}N_{4,5}$, of each AE spectra from pure SnO_2 and metallic Sn were broken down to two Gaussians. Peak widths for the Gaussians are determined from the curve fitting, so as to give the same value for the both Gaussians representing $M_5N_{4,5}N_{4,5}$ and $M_4N_{4,5}N_{4,5}$ within an MNN doublet. The peak separation of these Gaussians within a doublet was put equal to the energy separation of $d_{3/2}$ and $d_{5/2}$ spin-orbit coupling states determined from the 3d X-ray photoelectron spectra, and their relative peak heights are fixed to 3:4 which is expected from the electron population densities for $d_{3/2}$ and $d_{5/2}$.

An example of Sn MNN integral Auger peak fitting applied to the third spectrum from the front shown in Fig. 2 is shown in Fig. 4. As found in the figure, Sn MNN Auger spectrum (a) is well fitted with two Gaussian doublets obtained from SnO_2 (b) and from metallic Sn (c). The relative heights between the two doublets representing oxidic and metallic tin were the only fitting parameter used in this fitting, and is determined so as to give smooth background (d) after the subtraction of the two doublets, (b) and (c). This procedure depends on the fact that the background spectrum in AES normally consists of inelastic contribution of the outcoming Auger electrons, and is predominantly a monotonously decreasing function of electron energy at AE peaks.[18]

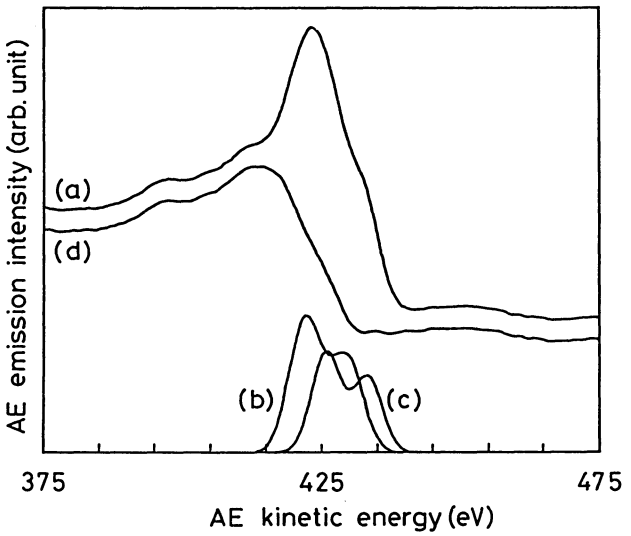

Fig. 4. An example of Sn MNN integral AE peak fitting by Gaussians: (a) integrated AE spectrum, (b) Gaussian doublets obtained from SnO_2 MNN spectrum, (c) Gaussian doublets obtained from metallic Sn MNN spectrum, and (d) subtracted spectrum (a−b−c) corresponding to baseline.

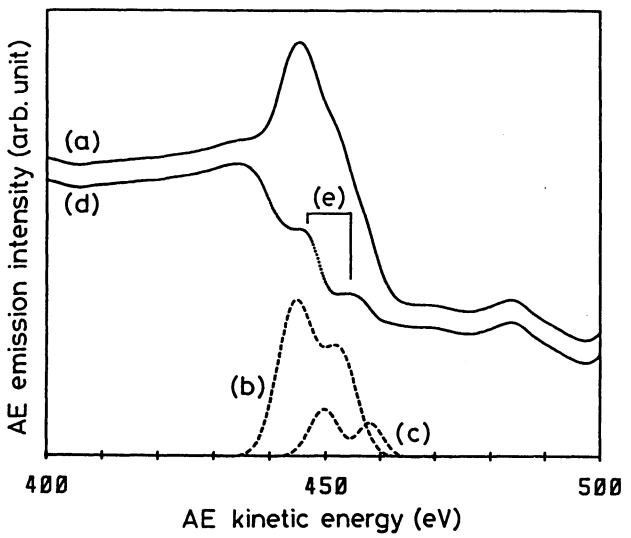

Fig. 6. An example of Sb MNN integral AE peak fitting by Gaussians: (a) integrated AE spectrum, (b) Gaussian doublets obtained from Sb_2O_5 MNN spectrum, (c) Gaussian doublets obtained from metallic Sb MNN spectrum, (d) subtracted spectrum (a−c−d) showing the presence of yet another doublet(e).

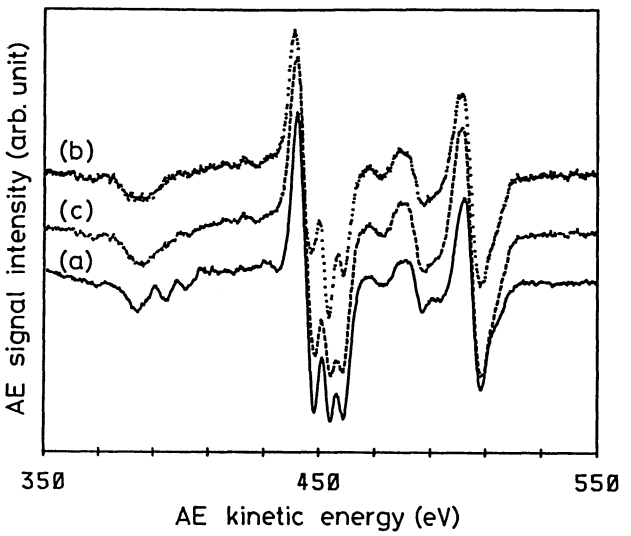

Fig. 5. An Example of Sb MNN differential AE spectrum curve fitting: (a) measured spectrum, (b) spectrum composed of standard Sb(V) and Sb(0) spectra, and (c) spectrum composed of standard Sb(V), Sb(III), and Sb(0) spectra.

In a similar fashion it is possible to curve-fit all the spectra shown in Fig. 2 with these two doublets. The result of the integral fitting is also shown in Fig. 3 (closed symbols). The integral and the differential curve fittings give almost identical results, indicating the soundness of the both methods employed here for AE spectral analysis.

Now the same fitting procedures were applied to Sb. In Fig. 5 an example of differential curve fitting is shown. This is the third spectrum from the front shown in Fig. 1. Spectrum (a) is the one obtained experimentally, and spectrum (b) is the best combination of the differential spectra obtained by linearly combining standard spectra from Sb_2O_5 and from metallic Sb. Comparison of the spectra (a) and (b) indicates that the linear combination of the Sb(V) and Sb(0) components is not satisfactory, and another component may be needed in order to simulate the experimental spectrum.

The presence of the third component is also suggested in the integral curve fitting, an example of which is shown in Fig. 6 for the same spectrum shown in Fig. 5. Here the subtraction of the two standard Gaussian doublets (b) and (c) obtained from Sb(V) and Sb(0), respectively, from the experimental spectrum (a) leaves yet another doublet (e), as indicated in the subtracted spectrum (d) in the figure.

This third Sb component suggested in Fig. 5 and apparent in Fig. 6 is obviously of intermediate valency between V and 0, as may be judged from the peak energy position in Fig. 6, and is most likely Sb(III). Search for a standard spectrum for this component was rather difficult, because commercial Sb_2O_3 gave AE spectrum almost identical to that of Sb_2O_5. This indicates that its surface is oxidized to Sb(V). Such surface oxidation seems to be a characteristic of Sb oxides: The present Sb_2O_5, actually Sb_6O_{13} in the bulk as determined by XRD, gives XP and AE spectra indicating the presence of single Sb component, Sb(V).

In order to obtain the standard spectrum for the third Sb component, we attempted in situ reduction of Sb oxide surface by electron bombardment. As indicated

earlier, we experienced many occasions in which Sb(V) was reduced just by being irradiated with high-energy electron beam. This reduction seems to proceed only to a certain extent, and the reduced surface gave well-defined, single component MNN AE doublet 1.6 eV higher than that of Sb(V). This in fact has an appearance of Sb(V) spectrum shifted 1.6 eV (referenced to O KLL). These facts indicate that this electron-reduced surface consists of single intermediate valency Sb, attributable to Sb(III). Thus this electron-irradiated spectrum was used as the standard for the third Sb species. It should be noted here that at this stage we do not have any other evidence for the formation of this Sb(III) surface species.

By adding this new differential spectrum to the other two standard spectra, the observed differential spectrum (Fig. 5, spectrum (a)) was successfully simulated, as may be exemplified by spectrum (c) in the figure. Integral spectra were also well fitted by the addition of this new component. It should be noted that the AES energy separation of 1.6 eV between the two oxidic components, Sb(V) and Sb(III), is much larger than that found in XPS, which is reported to be in the range of 0.5 to 1 eV.[8-10]

Thus in the course of thin Sb oxide reduction two oxidic and one metallic species were differentiated by AES. Using the fitting parameters thus obtained, the changes of the surface composition during ion bombardment of oxidized Sb metal is performed, and shown in Fig. 7. Certain discrepancies were found in the figure between the surface compositions deduced from the integral and from the differential fittings. This is probably due to the uncertainties involved in the AE spectral parameters for the Sb(III) component. The uncertainties are apparently higher for the integral curve fitting, because it involves more data processing than the differential procedure, and it also involve rather arbitrary judgement on the baseline.

Nevertheless, Fig. 7 shows how the oxidized Sb surface responds to the successive ion bombardment. While the amount of the highest valency Sb monotonously decreases, intermediate valency Sb first increases with ion bombardment time and then decreases, and at the same time the amount of the metallic state species monotonously increases. The behavior of the intermediate valency Sb is apparently of that of intermediate reaction product, indicating that the ion bombardment reduction proceeds from Sb(V) to Sb(III) to Sb(0). This behaviour is also explainable if one considers three-layered surface consisting of a top Sb(V) layer, a middle Sb(III) layer and a bottom Sb(0) layer. In this case ion bombardment successively sputters off the three layers, giving the depth profile shown in Figs 7.

Determination of Sb Average Valency in Mixed Oxides. With the curve fitting parameters obtained above, it is possible to construct composit spectra for Sb oxides in which known amount of Sb(V) and Sb(III) components are mixed, and then construct a plot giving the relation between the Sb MNN AES peak position and the average Sb valency. The plot thus constructed is given in Fig. 8. Here the differential method which seems to be more reliable of the two was employed, and the AE kinetic position is expressed as the crosspoint where the differential spectrum intersects with the abscissa.

The importance of such a plot given in Fig. 8 lies in the fact that it provides simple and quick method for the determination of average Sb oxidation number at the surface of mixed Sb oxide materials. For the bulk such information is obtainable by Mössbauer spectroscopy, although for the surface we have to rely on the peak fitting of either AES or XPS data as we have seen above. Utilizing this plot we determined the Sb average valency for several Sb-Sn mixed oxide catalysts,

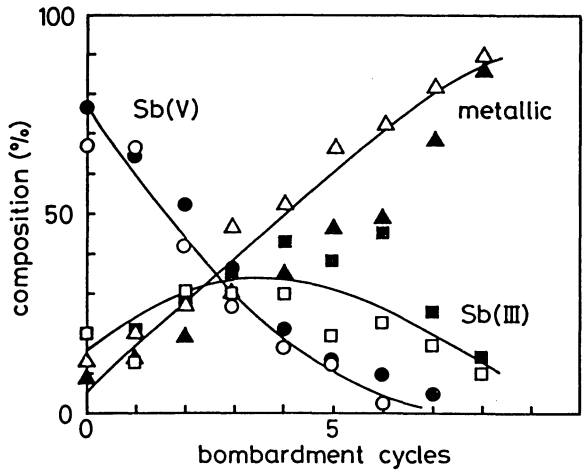

Fig. 7. Reduction behavior of oxidized Sb metal surface by ion bombardment analyzed by the two curve fitting methods. Open symbols: differential method; closed symbols: integral method.

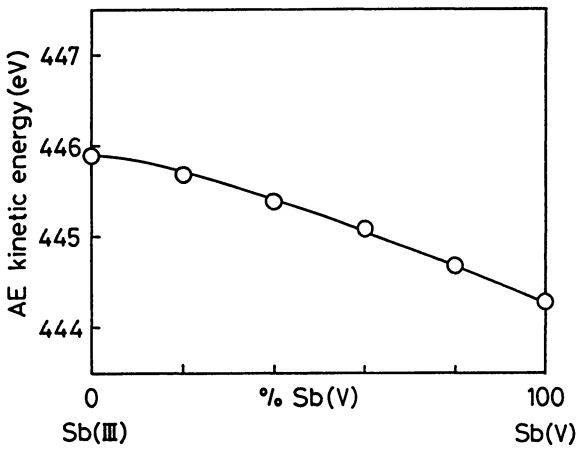

Fig. 8. The simulated relation between the AE peak position and the surface Sb(V) content in Sb(V)–Sb(III) mixed oxides using the differential method. The plotted AE kinetic energy positions are those of crosspoints.

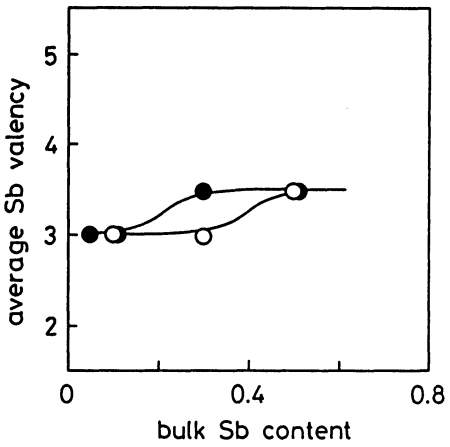

Fig. 9. Average valency of Sb in two Sn–Sb–O mixed oxide catalyst series determined by using Fig. 8. Open symbols: series A; closed symbols: series B.

shown in Fig. 9 as the function of bulk Sb/Sn ratio. Either series A and B catalysts seems to show V–III mixed state at heigher bulk Sb content, whereas at lower Sb content Sb(III) state is dominant. Due to the difference in preparation procedure and probably due to the resulting particle size difference,[2] series A catalysts (open circles) tend to give lower Sb valency than series B catalysts (closed circles) at similar bulk Sb content.

References

1) F. J. Barry, "Advances in Catalysis," Academic Press, New York (1981), Vol. 30, p. 97.
2) T. Ono, T. Yamanaka, Y. Kubokawa, and M. Komiyama, *J. Catal.*, **109**, 423 (1988).
3) Z. M. Jarzebski and J. P. Marton, *J. Electrochem. Soc.*, **123**, 199c; 299c (1976).
4) A. W. C. Lin, N. R. Armstrong, and T. Kuwana, *Anal. Chem.*, **49**, 1228 (1977).
5) R. A. Powell, *Appl. Surf. Sci.*, **2**, 397 (1979).
6) A. J. Bevolo, J. D. Verhoeven, and M. Noack, *Surf. Sci.*, **134**, 499 (1983).
7) W. E. Morgan, W. J. Stec, and J. R. Van Wazer, *Inorg. Chem.*, **12**, 953 (1973).
8) T. Birchall, J. A. Connor, and I. H. Hillier, *J. Chem. Soc., Dalton Trans.*, **1975**, 2003.
9) A. F. Orchard and G. Thornton, *J. Chem. Soc., Dalton Trans.*, **1977**, 1238.
10) F. Garbassi, *Surf. Interface Anal.*, **2**, 165 (1980).
11) M. Komiyama, Y. Ogino, M. Goto, and Y. Akai, *J. Chem. Soc., Faraday Trans. 2*, **79**, 1719 (1983).
12) M. Komiyama, H. Tsukamoto, and Y. Ogino, *J. Solid State Chem.*, **64**, 134 (1986).
13) L. E. Davis, N. C. MacDonald, P. W. Palmberg, G. E. Riach, and R. E. Weber, "Handbook of Auger Electron Spectroscopy," 2nd ed, Physical Electronic Ind., Eden Prairie (1978).
14) T. Ono, M. Kiryu, M. Komiyama, and R. L. Kuczkowski, *J. Catal.*, **127**, 698 (1991).
15) P. Sen, M. S. Hegde, and C. N. R. Rao, *Appl. Surf. Sci.*, **10**, 63 (1982).
16) P. T. Dawson and N. A. Burke, *J. Electron Spectrosc. Relar. Phenom.*, **31**, 355 (1983).
17) P. T. Dawson and K. K. Tzatzov, *Surf. Sci.*, **149**, 105 (1985).
18) N. Rosenberg, M. Tholomier, E. Vicario, and N. Doghmane, *Surf. Sci.*, **254**, 289 (1991).